Development of a High-Resolution and Depth-of-Interaction Capable Detector for Time-of-Flight PET

Srilalan Krishnamoorthy, *Member, IEEE*, Rony I. Wiener, Madhuri Kaul, Joseph Panetta, Joel S. Karp, *Senior Member, IEEE* and Suleman Surti, *Senior Member, IEEE*

***Abstract*–PET with its quantitative powers is becoming increasingly popular in the clinic. While the detector spatial resolution and sensitivity directly affect its ability, it has been shown that including the time-of-flight information further enhances its powers. Currently numerous approaches are being pursued to improve spatial resolution and timing, but most involve trade-offs. We describe here the development of a high-resolution PET detector with time-of-flight capabilities. The detector design is based on our previously developed pixelated Anger-logic detector where an array of individual crystals is readout by an array of larger photomultiplier tubes (PMTs) coupled to it via a light-guide. Depth-of-interaction (DOI) measurement in this design is accomplished by making use of a dual crystal-layer offset relative to each other. With a target spatial resolution of 1-2 mm, we have carefully evaluated the performance of several 1.5 x 1.5 and 2.0 x 2.0 mm^2 and 10-20 mm long LYSO crystals readout by several appropriately sized PMTs. Experiments and simulations were used to investigate the design, and optimize performance of the detector. An experimental prototype using a single 8 x 7 array of 1.5 x 1.5 x 12 mm^3 LYSO crystals readout by a 7-PMT array of the Hamamatsu R4124 PMTs was developed. A high-speed waveform sampling data acquisition system based on the DRS4 switched-capacitor that digitizes data at 5 GS/s was also built. Experimental evaluations demonstrate that the detector provides very good timing and also successfully discriminates 1.5 x 1.5 mm^2 cross-section scintillation crystals. Bench-top timing measurements with a dual-layer detector demonstrate that relatively good timing can be maintained in a stacked crystal arrangement, suggesting the feasibility for extending the approach to incorporate DOI with this design.**

I. Introduction

While the importance of detector spatial resolution and sensitivity on overall PET performance are well understood, including the time-of-flight (TOF) information adds significantly to the quantitative powers of PET [1–3]. With the resurfacing of TOF-PET in this past decade have been significant advances in developing high performance detectors [4]. Most of the detector advances though have performance trade-offs, and researchers are still exploring ways to develop a detector with high spatial and temporal resolutions. We describe here the development of a high-spatial resolution scintillation detector with time-of-flight capabilities. While such a detector would have numerous applications, we are particularly interested in demonstrating its relevance in a limited-angle tomograph where the TOF data would help eliminate artifacts arising from the limited angular sampling [5].

Manuscript received November 15, 2011. This work was supported in part by the National Institutes of Health under grants R01EB009056 (National Institute of Biomedical Imaging and Bioengineering), R01CA113941 (National Cancer Institute) and a research agreement with Saint-Gobain crystals.

Srilalan Krishnamoorthy (E-mail: srilalan@mail.med.upenn.edu), Joseph Panetta and Suleman Surti (E-mail: surti@mail.med.upenn.edu) are with the Department of Radiology, University of Pennsylvania, Philadelphia, PA 19104, USA. Rony I. Wiener and Madhuri Kaul are with the Department of Physics and Astronomy at the University of Pennsylvania. Joel S. Karp (E-mail: joelkarp@mail.med.upenn.edu) is with the Departments of Radiology and Physics & Astronomy at the University of Pennsylvania.

II. Materials and Methods

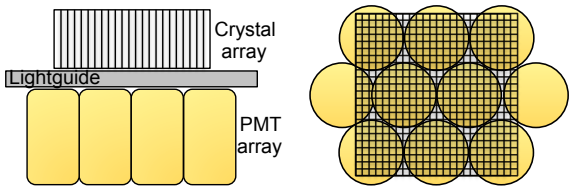

Fig. 1. A schematic of the proposed high-resolution TOF PET detector: The detector design is based on our previously developed pixelated Anger-logic detector [6] wherein an array of individual crystals are readout by a hexagonal arrangement of PMT coupled to it via a single continuous light-guide. *Left*: side view, *Right*: top view.

A. Detector design

The detector design is based on our previously developed pixelated Anger-logic detector [6] where an array of individual crystals is readout by an array of larger PMTs coupled to it via a light-guide (illustrated in Fig.1). The light-spread from a single gamma interaction is limited to a 7-PMT cluster arranged in a hexagonal arrangement. This type of detector has been extensively studied previously and successfully used to develop a non-TOF PET scanner (A-PET) where an array of 2 x 2 x 10 mm^3 crystals were readout by 19 mm PMTs [7].

PMT Model (diameter, mm)	Quantum Efficiency (at 420 nm)	Transit time spread (ns)	Rise time (ns)
R4998 (25)	22	0.16	0.70
R3478 (19)	27	0.36	1.30
R4124 (13)	25	0.50	1.10
R1635 (10)	25	0.5	0.80

Table I. A comparison of select commercially available fast photomultiplier tubes appropriate for our design of a high-resolution time-of-flight PET detector. All the above tubes are manufactured by Hamamatsu Photonics [8].

With a spatial-resolution of the order of 1-2 mm in mind, we carefully evaluated crystals with smaller cross-sections (1.4 x 1.4 mm^2 & 1.95 x 1.95 mm^2). To increase detector sensitivity,

crystal lengths of 12-15 mm were chosen. Several fast PMTs, appropriately sized to read-out the smaller cross-sectional crystals were also procured (Table I).

B. Timing with small cross-sectional scintillation crystals

We are developing a TOF PET detector and it is imperative that the detector has good timing resolution. Since the small-cross-section and long crystals have inherently poorer light collection efficiency we tried to carefully evaluate the timing performance of several small and long crystals coupled with appropriate fast PMTs listed earlier. Each of the crystals were wrapped with Teflon on five sides and grease-coupled directly to each of the different PMTs. While a detailed study of the crystal surface finish optimization and its effects on timing resolution is in order (and currently underway), here we report on the measurements with diffuse and polished surface finish on the entrance face of the scintillator. For comparison, we also include measurements with a 4 x 4 x 22 mm^3 LSYO crystal that is similar in size to the crystals used in some commercial TOF-PET scanners.

Hamamatsu PMT model	Coincidence timing resolution (ps, FWHM)			
	4 x 4 x 22 mm^3 LYSO (polished surfaces)	1.95 x 1.95 x 15 mm^3 LYSO (polished surfaces)	1.4 x 1.4 x 12 mm^3 LYSO (polished surfaces)	1.4 x 1.4 x 12 mm^3 LYSO (diffused entrance, other faces polished)
R4998	245	250	284	280
R3478	305	300	300	285
R4124	315	300	285	280
R1635	230	250	240	230

Table II. Coincidence timing measurements for different (size) individual LYSO crystals placed directly on several test PMTs outlined in Table I. The timing measurements indicate that comparable or better timing can be achieved even with small and long scintillation crystals. Measurements with a 4 x 4 x 22 mm^3 LYSO crystal are also shown for comparison. All measurements are precise within ±5% and were performed with a 511 keV ^{22}Na source and a small $LaBr_3$ (5% Ce), XP20D0 PMT combination as the reference detector. Two such reference detectors for this measurement had a coincidence timing of 225 ps FWHM.

Our timing measurements (shown in Table II) indicate that reading the small cross-sectional crystals with fast PMTs yields comparable (or better) timing than presently achieved with crystals used in clinical whole-body time-of-flight scanners [9-11]; indicating their suitability for building a high spatial resolution time-of-flight PET detector.

C. Waveform sampling data-acquisition

With a consistent improvement in the achievable timing resolution of modern-day detectors, researchers are soon approaching limits where digital signal processing techniques offer flexibility and superior performance in comparison with traditional processing schemes [12-13].

Given the versatility, we assembled a waveform sampling data acquisition system to acquire and process data from our prototype detectors. The DAQ was based on the CAEN N6742, which is a NIM module housing 16 channels based on the DRS4 chip [14-16]. Each channel on the digitizer has 1 Vp-p dynamic range and can be digitized at 5GS/s with 12-bit precision. Data from the detector is digitized with minimal use of NIM electronics. The digitized data is transferred to a host computer via USB and all analysis is performed offline via custom code developed in MATLAB. Fig. 2 shows the schematic of the data acquisition system.

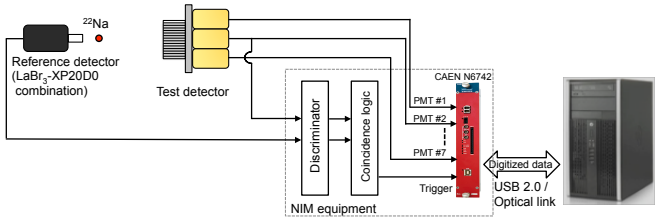

Fig. 2. A schematic of the detector setup and data acquisition system used to evaluate detector performance. Data was acquired with minimal NIM electronics and a waveform sampling DAQ based on the CAEN-N6742 module [14]. The N6742 digitizer is based on the DRS4 chip [15-16] and provides 16 channels that can each be digitized at 5 GS/s. A small $LaBr_3$ (5% Ce), XP20D0 PMT combination was used as the reference detector.

III. Initial Simulation Studies

To initially evaluate the positioning capabilities of the proposed high-resolution detector, we performed Monte Carlo studies using our *Montecrystal* program [6]. A single array of 1.5 x 1.5 x 15 mm^3 LYSO crystals were readout by a hexagonally packed arrangement of 13 mm and 19 mm PMT respectively. Simulations were used to choose a light-guide thickness such that the light-spread function at the center of the detector did not extend beyond the 7-PMT-cluster and suggested the use of a 6 and 9 mm thick light-guide to couple the 13 and 19 mm PMTs respectively. A narrow beam of 511 keV photons was incident on the detector and the interaction locations were measured with Anger-logic using the 7 PMTs. Fig. 3 show position spectra from a region of the detector directly over the central PMT. While both the PMTs could help discriminate the 1.5 mm wide crystals, as expected the 13 mm PMTs provide superior crystal discrimination when compared with the 19 mm PMTs.

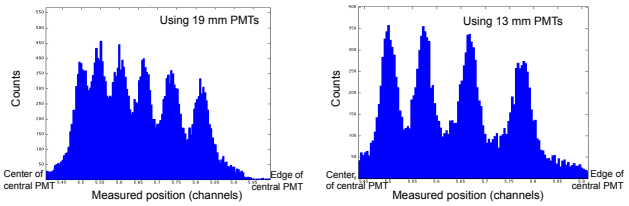

Fig. 3. Simulation studies demonstrating the resolving capabilities of the detector: An array of 1.5 x 1.5 mm^2 LYSO crystals were readout by a hexagonal arrangement of the 19 mm and 13 mm PMTs respectively. Shown above are position spectra from the scintillation crystals laying directly over one half of the central PMT in the detector readout by 19 mm PMTs (*left;* see six 1.5 mm wide crystals) and 13 mm PMTs (*right*; see four 1.5 mm wide crystals) respectively.

IV. Experimental Evaluation of Prototype Detector Performance

Since the 13 mm PMTs showed superior detector performance, to demonstrate feasibility, an experimental prototype was developed using an 8 x 7 array of 1.5 x 1.5 x 12 mm^3 LYSO crystals (which were readily available) readout by an array of 13 mm PMTs (R4124). As suggested by simulations a 6.2 mm light-guide was used between the

crystal-array and PMTs. Fig. 4 shows a photo of the crystal array, PMT and the assembled detector. To evaluate detector performance, a 511 keV ^{22}Na was placed between the prototype detector and a reference detector consisting of a small $LaBr_3$ (5% Ce) directly coupled to a Photonis XP20D0 PMT. All seven R4124 PMTs were biased with a single bias-line set to 1200 V. PMT signals from the test and reference detector were digitized with the CAEN N6742 and stored to disk. All data was processed offline. Signals from all seven PMTs were combined with Anger-logic to determine the crystal interaction location within the array.

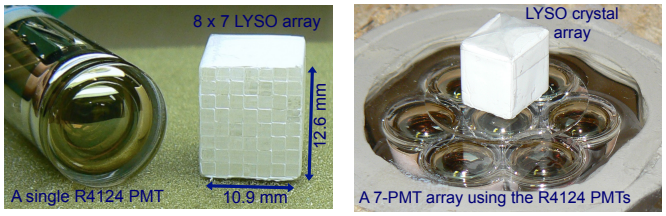

Fig. 4. *Left*: Photo of a single 13 mm diameter R4124 PMT and 8x7 array of LYSO crystals (1.5x1.5x12 mm^3 each) used to build a first prototype detector. *Right*: Assembled prototype detector showing the crystal array and the array of seven R4124 PMTs used to readout the crystal array. A 6.2 mm thick light-guide was used between the crystal-array and PMTs.

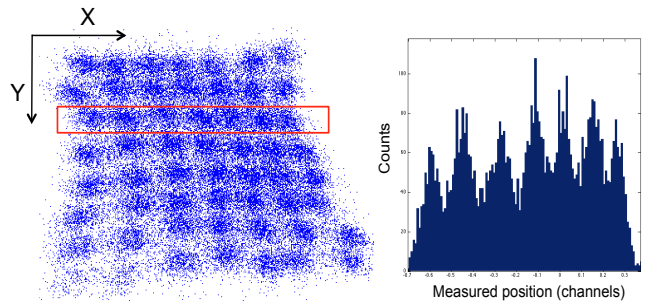

Fig. 5. *Left*: Flood histogram acquired from the prototype detector with a ^{22}Na source and the waveform sampling DAQ described earlier. Signals from all 7-PMTs were combined with Anger-logic to measure the interaction location within the array. *Right*: A profile (indicated in red) drawn through a single row of the acquired flood histogram. All crystals within the array can be clearly resolved demonstrating the spatial resolution of the detector.

Fig. 5 shows the flood map from one such acquisition. All 56 crystals within the array can be resolved, demonstrating the spatial resolution of the detector. While all the crystals in the flood map can be resolved, the results do not exactly match with predictions from simulations. Optimizing the surface finish and reflector properties of the crystal array should improve crystal discrimination. Another concern with the current prototype is the limited active-area (~60%) of the R4124 PMT, which affects the sampling of the light-spread-function within the detector. Also shown in Fig.5 is a profile of the position spectra from a row of crystals near the center of the detector. To measure energy and coincidence timing resolution, the respective spectrum was calculated by selectively gating on individual crystals within the flood-map. Fig. 6 shows sample energy and timing spectrum for interactions occurring in a crystal near the center of the detector; energy resolution of 14 % FWHM and timing resolution of 350 ps FWHM were measured for that single crystal. Fig. 7 is a histogram of the energy and timing resolution for individual crystals from the 8 x 7 LYSO array. An average energy resolution of 15.5 % FWHM and timing resolution of 380 ps was measured for the detector. Accounting for the timing contributions from the reference detector (247 ps FWHM for two reference detectors in coincidence) an average coincidence timing resolution of 475 ps is predicted for two such detectors in coincidence.

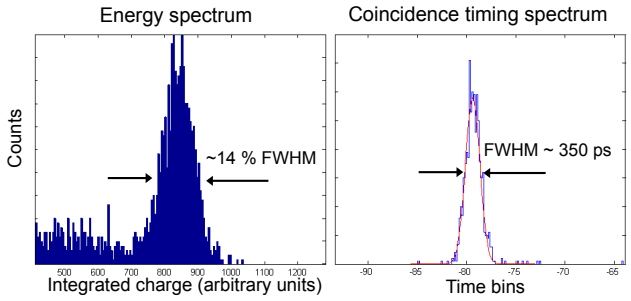

Fig. 6. Typical energy (*left*) and coincidence timing (*right*) spectra from a single 1.5 x 1.5 x 12 mm^3 LYSO crystal located near the center of the entire 8 x 7 crystal array.

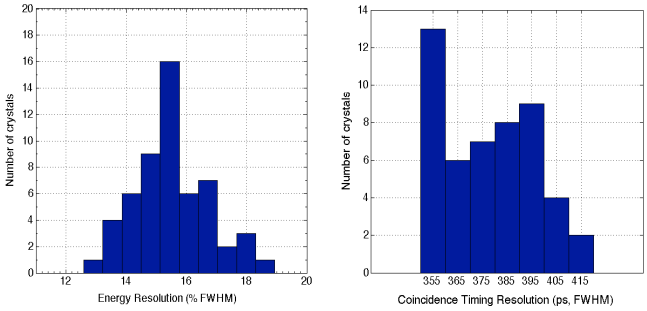

Fig. 7. Histogram of the energy (*left*) and timing resolutions (*right*) measured for individual crystals from the 8 x 7 LYSO array: An average energy resolution of 15.5 % FWHM was measured for the entire detector. A best time resolution of 350 ps FWHM, and an average time resolution of 380 ps FWHM were measured. Accounting for the timing contribution from the reference detector (247 ps FWHM for two reference detectors in coincidence), an average coincidence time resolution of 475 ps can be measured for two such detectors in coincidence.

The above detector measurements are consistent with our previous experiences [17], which have shown a 10-20% loss in coincidence timing resolution when moving from a single-crystal placed directly over a single PMT to an array of crystals coupled to a PMT-array via a light-guide. Carefully minimizing the light-loss by optimizing the light-guide thickness should further help in improving detector performance.

V. Depth-of-Interaction Studies

Experimental studies have already demonstrated the ability of the detector to decode small cross-section crystals, and offer good energy and timing resolutions. Since we are exploring its first application for a limited-angle TOF scanner for clinical imaging, we make use of long (10-20 mm) crystals

to increase the scanner sensitivity. The longer crystals though are prone to parallax errors, especially in a small ring diameter scanner e.g. breast scanner. The addition of depth-of-interaction (DOI) information should help in improving overall performance of the scanner. DOI information can be measured by making use of a dual-layer detector. In this configuration the additional layer could be coupled end-on-end (phoswich) or could be offset relative to the first layer in 1-D or 2-D. While the availability of a fully digital DAQ should in principle allow implementing a phoswich detector, the intrinsically different decay times and light-output needed for the two layers can cause significant variations in timing resolution. While this would require a more careful investigation, for this work we investigate the feasibility of using a dual-offset layer for DOI measurements.

A. Simulation studies

The simulations used earlier (Section III) were used again to evaluate the DOI capabilities of the detector. A two-layer detector consisting of 1.5 x 1.5 mm^2 LYSO crystals, 7 mm thick at the near-end and 10 mm thick (close to the PMT-array) was modeled and readout by a 6 mm light-guide and an array of 13 mm PMTs. Fig. 8 shows a flood map of the detector response from a portion of the crystals directly over the central PMT. The flood map demonstrates reasonable crystal discrimination for crystals from both the layers.

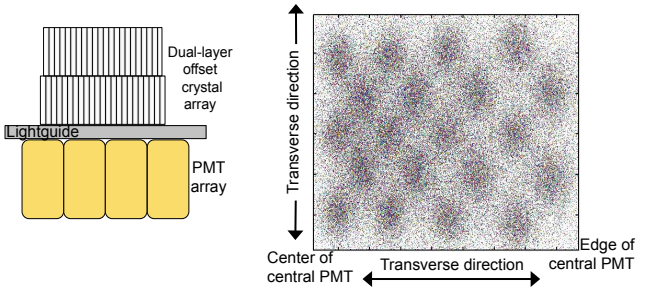

Fig. 8. *Left*: Schematic of a dual-layer detector extended to provide depth-of-interaction information. *Right*: Simulations were used to evaluate the DOI discrimination capabilities of the detector. A two-layer detector comprising of a 1.5 x 1.5 mm^2 LYSO crystals (7 mm thick layer at the entrance face, and a 10 mm thick layer near the PMT-array) was readout by an array of the R4124 PMTs coupled to a 6 mm light-guide. The two crystal layers were offset relative to each other in 2-D. Figure shows expected flood map from a region directly over the central PMT.

While this suggests feasibility of incorporating DOI in the above detector, the flood map obtained through experimental evaluations (Section IV) suggests that improvements are necessary to accommodate the additional crystal layer with the current prototype. We are currently investigating methods to improve performance of the prototype detector. Since the dead area surrounding the photocathode of the R4124 PMT is of significance we are exploring the use of a multianode PMT. The higher active-area and improved sampling of the multianode PMT should help improve detector performance. Timing measurements with a single 1.4 x 1.4 x 12 mm^3 LYSO crystal coupled to a Hamamatsu H8500 multianode PMT and the previously described reference detector (Table I) provides a timing of 320 ps FWHM. Also, initial flood-map measurements with the previously described 8 x 7 crystal array coupled to a H8500 PMT improves crystal discrimination (not shown here).

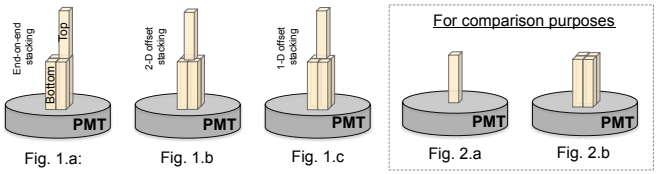

Fig.	Crystal	Beam Direction	Coincidence time resolution (ps, FWHM)	Light collection (arbitrary units)	Energy resolution (% FWHM)
1.a	Stacked; end-on-end	Top crystal, side-on	375	135	16
		Bottom crystal, side-on	330	177	23
1.b	Stacked; 2-D offset	Top crystal, side-on	400	130	18.7
1.c	Stacked; 1-D offset	Top crystal, side-on	370	146	16.3
2.a	Single crystal, teflon wrapped on all sides	Head-on	300	230	12.9
2.b	2 x 2 array, teflon wrapped on all sides	Head-on	305	220	16
		Side-on	296	223	16
2.b	2 x 2 array, long sides teflon wrapped	Head-on	325	180	27
		Side-on	310	190	15.5

Fig. 9. *Top*: Illustration of the various dual-layer detector configurations under which a careful evaluation of detector timing resolution was performed. *Bottom*: Bench-top measurements with readily available individual crystals (15 mm long each) indicate that good timing can be achieved with two separate, stacked layers of crystals in the detector. All crystals used (1.95 x 1.95 x 15 mm^3 LYSO) had polished surfaces and were Teflon wrapped. All measurements are accurate within ±5% and were performed with a 511 keV ^{22}Na source and a small $LaBr_3$ (5% Ce), XP20D0 PMT combination as the reference detector. Two such reference detectors had a timing of 225 ps FWHM. Since the head-on measurement (gamma source normal to the short-face of the crystal) includes effects from the various depths (along the length of the crystal) along which the gamma-ray interacts, the measurements were also performed with the beam in a side-on position (normal to its long side). For the side-on measurements, the beam was about 5 mm wide. The measurements demonstrate that good timing can be obtained with a dual-layer crystal array wherein the two layers are offset relative to each other.

B. Timing with a dual-layer scintillation detector

While the concept of using a stacked layer of scintillators to decode DOI has been experimentally demonstrated earlier [18-19], a careful evaluation of the timing properties of the detector has not been performed. Our primary goal was to develop a TOF detector with high spatial resolution. Hence we tried to evaluate the relative loss in timing when employing a dual crystal-layer to include DOI-decoding. Since the goal of the study was to primarily evaluate the relative timing loss in crystals arranged in a dual-layer configuration, a 2 x 2 array with readily available 1.95 x 1.95 x 15 mm^3 polished, LYSO crystals was assembled. All the four crystals were Teflon wrapped and used on the bottom layer (closer to the PMT) of a dual-layer crystal array (Fig. 9). For simplicity of fabrication, the exposed short-sides of all the four crystals were bare and had no reflector on them. An identical single LYSO crystal, Teflon wrapped on all five sides was used as the top-layer (i.e. away from the PMT). The various detector configurations under which timing performance was evaluated (phoswich, 2-D stacking and 1-D stacking) are illustrated in Fig. 9 (1.a, 1.b and 1.c). For comparison purposes, we also separately

benchmarked the timing of the individual 2 x 2 array and the single crystal used on the top-layer. To help understand the timing losses from the exposed top-surfaces of the bottom-layer the benchmarking was performed with and without Teflon on its top surfaces. Since each crystal was long (15 mm), and the DOI of the gamma-ray would affect the timing measurements, the measurements were performed with the beam in the head-on (normal to the crystal-face) and side-on (normal to the long side) directions.

Measurements demonstrate that good timing can be obtained with a stacked crystal arrangement (Fig. 9), indicating their suitability to decode DOI in the proposed high-resolution TOF detector design. We show that there are systematic losses in timing when transitioning from a single crystal layer to a stacked-layer. Better timing is achieved from a single layer when compared with the same crystal used on the bottom-layer of a dual-layer detector. This could be explained by the increase in the effective length of the crystal (30 mm versus 15 mm originally). Further degradation of the timing is observed from the top-layer. However, as the total crystal-length in the final design is expected to be shorter than 30 mm, we expect better timing performance than measurements presented here.

VI. Conclusions

This paper discusses the development of a high-spatial resolution detector with time-of-flight capabilities. With a target spatial resolution of 1-2 mm we initially studied the timing performance of several small cross-sectional crystals readout by appropriately sized fast PMTs. Subsequently a first prototype detector comprising of a 8 x 7 array of 1.5 x 1.5 x 12 mm^3 LYSO crystals readout by a hexagonally packed arrangement of seven Hamamatsu R4124 PMTs was developed. Experimental evaluations demonstrate the ability of the detector to decode the small (cross-section) and long crystals while maintaining sufficiently good timing (475 ps on average for two such detectors in coincidence) and energy resolution (15.5 % FWHM on average). We also evaluated the initial feasibility of extending the detector to incorporate DOI-decoding. Bench-top measurements with individual crystals indicate that reasonably good timing can be achieved even with two separate, stacked layers of crystals in the detector.

References

[1] T.F. Budinger, "Time-of-Flight positron emission tomography: status relative to conventional PET," *J. Nucl. Med.*, vol. 24, pp. 73-76, 1983.

[2] S. Surti, J.S. Karp, L.M. Popescu, M.E. Daube-Witherspoon and M. Werner, "Investigation of time-of-flight benefit for fully 3-D PET," *IEEE Trans. Nucl. Sci.*, vol. 25, no. 5, pp. 529-538, May 2006.

[3] J.S. Karp, S. Surti, M.E. Daube-Witherspoon and G. Muehllehner, "Benefits of Time-of-Flight: experimental and clinical results," *J. Nucl. Med.*, vol. 49, no. 3, pp. 462-470, March 2008.

[4] W.W. Moses, "Time of flight in PET revisited," *IEEE Trans Nucl Sci.*, vol. 50, no. 5, pp. 1325-1330, 2003.

[5] S. Surti and J.S. Karp, "Design considerations for a limited-angle, dedicated breast, TOF PET scanner," *Phys. Med. Biol.*, vol. 53, no. 11, pp. 2911-2921, 2008.

[6] S. Surti, J.S. Karp, R. Freifelder and F. Liu, "Optimizing the performance of a PET detector using discrete GSO crystals on a continuous lightguide," *IEEE Trans. Nucl. Sci.*, vol. 47, pp. 1030-1036, 2000.

[7] S. Surti, J.S. Karp, A.E. Perkins, R. Freifelder and G. Muehllehner, "Design evaluation of A-PET: A high sensitivity animal PET camera," *IEEE Trans. Nucl. Sci.*, vol. 50, no.5, pp. 1357-1363, 2003.

[8] http://www.hamamatsu.com

[9] S. Surti, A Kuhn, M.E. Werner, A.E. Perkins, J. Kolthammer and J.S. Karp, "Performance of Philips Gemini TF PET/CT scanner with special consideration for its Time-of-Flight capabilities," *J. Nucl. Med.*, vol. 48, pp. 471-480, 2007.

[10] B.W. Jakoby, Y. Bercier, M. Conti, M.E. Casey, B. Bendriem and D.W. Townsend, "Physical and clinical performance of the mCT time-of-flight PET/CT scanner," *Phys. Med. Biol.*, vol. 56, pp. 2375-2389, 2005.

[11] V. Bettinardi, L. Presotto, E. Rapisarda, M. Picchio, L. Gianolli, and M.C. Ginardi, "Physical performance of the new hybrid PET/CT Discovery-690," *Medical Physics*, vol. 38, no. 10, pp. 5394-5411, 2011.

[12] R.I. Wiener, S. Surti, C.C.M. Kyba, M.F. Newcomer, R. Van Berg and J.S. Karp, "An investigation of waveform sampling for improved signal processing in TOF PET," *IEEE Nuclear Science Symposium and Medical Imaging Conference*, pp. 4101-4105, 2008.

[13] J.-F Genat, G. Varner, F. Tang and H. Frisch, "Signal processing for picosecond resolution timing measurements," *Nucl. Instruments and Methods in Physics Research Section A*, vol. 607, no. 2, pp. 387-393, August 2009.

[14] http://www.caen.it/csite/CaenProd.jsp?idmod=652&parent=12

[15] S. Ritt, "Design and performance of the 6 GHz waveform digitizing chip DRS4," *IEEE Nuclear Science Symposium and Medical Imaging Conference*, pp. 1512-1515, 2008.

[16] http://drs.web.psi.ch/

[17] A. Kuhn, S. Surti, J.S. Karp, P.S. Raby, K.S. Shah, A.E. Perkins and G. Muehllehner, "Design of a lanthanum bromide detector for Time-of-Flight PET," *IEEE Trans. Nucl. Sci.*, vol. 51, no.5, pp. 2550-2557, 2004.

[18] N. Zhang, C.J. Thompson, D. Togane, F. Cayouette, K.Q. Nguyen and M.L. Camborde, "Anode position and last dynode timing circuits for dual-layer BGO scintillator with PS-PMT based modular PET detectors," *IEEE Trans Nucl Sci.*, vol. 49, no. 5, pp. 2203-2207, 2002.

[19] T. Tsuda, H. Murayama, K. Kitamura, T. Yamaya, E. Yoshida, T, Omura, H. Kawai, N. Inadama and N. Orita, "A four layer depth of interaction detector block for small animal PET," *IEEE Trans Nucl Sci.*, vol. 51, no. 5, pp. 2537-2542, 2003.